RSC Advances

PAPER

View Article Online
View Journal | View Issue

Cite this: *RSC Adv.*, 2017, **7**, 25828

The synergistic effect of type I collagen and hyaluronic acid on the biological properties of Col/HA-multilayer-modified titanium coatings: an *in vitro* and *in vivo* study

Haiyong Ao,†[ab] Chucheng Lin,†[c] Binen Nie,[d] Shengbing Yang,[d] Youtao Xie,[b] Yizao Wan[a] and Xuebin Zheng*[b]

Type I collagen and hyaluronic acid are both the main components of bone extracellular matrix, and play important roles in regulating a cell's behavior. In this study, the synergistic effects of type I collagen (Col) and hyaluronic acid (HA) on the biological properties of Col/HA-multilayer-modified titanium coatings were investigated. *In vitro*, the results of human mesenchymal stem cells culture indicated that Col/HA-multilayers-modified titanium coatings (TC-AA(C/H)$_6$) could better improve a cell's adhesion, proliferation, and differentiation, compared with collagen-modified titanium coatings (TC-AAC) and hyaluronic acid-modified titanium coatings (TC-AAH). *In vivo*, the micro-CT images indicated that bone trabecula around TC-AA(C/H)$_6$ were significantly more than with TC-AAC and TC-AAH. The fluorescence micrograph showed more active new bone formation around implants in TC-AA(C/H)$_6$ group than in the TC-AAC and TC-AAH groups in the first month. Measurement of the bone-implant contact on the histological sections indicated there was significantly good osteointegration around TC-AA(C/H)$_6$ implants than with the other two modified titanium coatings. All of these results demonstrated that there exists favorable synergistic effects of type I collagen and hyaluronic acid.

Received 26th November 2016
Accepted 23rd March 2017

DOI: 10.1039/c6ra27364e

rsc.li/rsc-advances

1. Introduction

The extracellular matrix (ECM) is a complex and dynamic network constituted by collagens, glycoproteins, glycosaminoglycan, and cytokines, which maintain tissue cohesion, provide physical support, and determine the mechanical properties of tissues.[1–3] ECM also forms a cell survival environment, as well as playing vital roles in regulating cell morphology, migration, proliferation, differentiation, and maturation.[4–7] Therefore, the components of ECM have become recognized as important building blocks for the creation of new biomaterials with utility in tissue engineering and regenerative medicine.

Many ECM components, such as type I collagen and hyaluronic acid (HA), have been widely used for biomaterials in a variety of forms, such as scaffolds,[8] hydrogels,[9] films,[10] and coatings on other biomaterials.[11] Type I collagen, as the main component of bone extracellular matrix, modulates various aspects of the cell behavior through the amino acid sequence arginine–glycine–asparagine (RGD) recognized by the integrin receptors of cells.[12–14] Except for combining the integrin receptors of cells, type I collagen also provides binding sites for other ECM components, such as fibronectin, vitronectin, laminin, and growth factors.[15,16] Hyaluronic acid (HA), one kind of glycosaminoglycan, is a ubiquitous component of the extracellular matrix of many tissues. HA plays an important role in tissue support, lubrication, and in the modulation of tissue viscoelasticity.[17] It also interacts with cell surface receptors CD44 and RHAMM to direct a wide spectrum of cell functions.[18,19] Furthermore, HA takes part in the building of proteoglycans by connecting core protein with non-covalent bonds.[20] Therefore, type I collagen and HA are frequently used with other ECM components to obtain better biological properties.[21–23]

Titanium (Ti) and titanium alloy-based biomaterials have been widely and successfully used as orthopedic and dental implants because of their good mechanical properties and biocompatibility.[24] Plasma-sprayed titanium coatings (TC) with rough surfaces and macroporous structures can improve the fixation of implants by promoting the growth of bone into the

[a]*School of Materials Science and Engineering, East China Jiaotong University, Nanchang, China 330013*

[b]*Key Laboratory of Inorganic Coating Materials, Shanghai Institute of Ceramics, Chinese Academy of Science, Shanghai, China 200050. E-mail: xbzheng@mail.sic.ac.cn*

[c]*State Key Laboratory of High Performance Ceramics and Superfine Microstructure, Shanghai Institute of Ceramics, Chinese Academy of Sciences, Shanghai, China 200050*

[d]*Shanghai Key Laboratory of Orthopedic Implants, Shanghai Ninth People's Hospital, Shanghai Jiao Tong University School of Medicine, Shanghai, China 200011*

† These authors contributed equally to this work.

coatings, thereby forming a mechanical interlock.[25] However, it does not have bone-inductive potential and cannot induce bone-bonding with living bone tissue because it is bioinert.[26] Therefore, many strategies, such as biochemical methods, have been used to improve the bioactivity of titanium-coated implants. The purpose of biochemical surface modification is to induce specific cell and tissue responses by immobilizing components of ECM.[27] In our previous literature,[28] a type I collagen/hyaluronic acid (Col/HA)-multilayer-film-modified TC with stability was fabricated by layer-by-layer covalent immobilization. We found that the biological properties of the Col/HA covalently-immobilized TC was better than that of the Col/HA-absorbed TC because of the improved stability. We also found that type I collagen and hyaluronic acid both could improve the osteoconduction and osseointegration of TC-based implants.[29,30] However, the synergistic effects of type I collagen and hyaluronic acid on the biological properties of Col/HA-multilayer-modified TC should be further studied.

The aim of this study was to investigate the synergistic effect of type I collagen and hyaluronic acid in Col/HA-multilayer-modified titanium coatings. Human mesenchymal stem cells (hMSCs) were employed to compare the ability of three kinds of modified titanium coatings: collagen-modified titanium coatings, hyaluronic acid-modified titanium coatings, and Col/HA-multilayer-modified titanium coatings. An *in vivo* study based on a rabbit model with a femur condyle defect was employed. Peri-implant bone regeneration and osseointegration of the bone-implant interface were investigated through micro-CT, fluorescence labeling of the new bone, and histological observation assays.

2. Materials and methods

2.1 Materials

Titanium coatings on Ti–6Al–4V plates of Φ 10 mm × 2 mm and Φ 34 mm × 2 mm and Ti rods of 2.6 mm × 10 mm (denoted as TC) were fabricated by vacuum plasma spraying (VPS, F4-VB, Sulzer Metco, Switzerland). Type I collagen (Col) from calf skin was obtained from Sigma-Aldrich, China. Hyaluronic acid (HA) was purchased from Bloomage Freda Biopharm CO., LTD., China. Silane-coupling agent aminopropyltriethoxysilane (APS) and *N*-hydroxysuccinimide (NHS) were obtained from Shanghai Sinopharm Chemical Reagent Corp., China. 1-Ethyl-3-(3-dimethylaminopropyl) carbodiimide (EDC) was produced by Tokyo Chemical Industry Co. LTD., Japan.

2.2 Preparation of the modified titanium coatings

Titanium coating samples were immersed in 5 M NaOH at 80 °C for 12 h, ultrasonically cleaned in deionized water, and then dipped in deionized water at 60 °C for 7 days with the water changed daily. After ultrasonic cleaning, the samples were dried under vacuum. Then, the samples were immersed in a boiling APS/toluene solution (APS concentration of 10%) for silanzation. After 12 h, the APS-coated samples were ultrasonically washed once in methanol and twice in deionized water, and then dried prior to further modification.

Type I collagen-modified titanium coatings (denoted as TC-AAC) were prepared as previously described.[31] Simply, the APS-coated samples were immersed in 1 mg ml^{-1} type I collagen/acetic acid (5 mM) solution including 2.5 mg ml^{-1} EDC and 0.63 mg ml^{-1} NHS, and reacted for 6 h. Preparation of the hyaluronic acid-modified titanium coatings (denoted as TC-AAH) was performed as for the TC-AAC, and the concentration of HA/acetic acid solution was also 1 mg ml^{-1}. Col/HA-multilayers-modified titanium coatings (denoted as TC-AA(C/H)$_6$) were manufactured by layer-by-layer covalent immobilization as previously described.[28] Briefly, the APS-coated samples were dipped into a collagen solution including 2.5 mg ml^{-1} EDC and 0.63 mg ml^{-1} NHS for 30 min, rinsed with deionized water, and then soaked into the HA solution including 2.5 mg ml^{-1} EDC and 0.63 mg ml^{-1} NHS for 30 min, followed by rinsing with deionized water. The cycle was repeated six times. After reaction, all the samples were ultrasonically cleaned with deionized water and dried under vacuum. To facilitate observation in ALP staining and with the Alizarin red staining assay, Col and HA were introduced onto the surface of Ti–6Al–4V plates instead of titanium coatings (denoted as Ti-AAC, Ti-AAH, and Ti-AA(C/H)$_6$, respectively).

2.3 *In vitro* study

2.3.1 Cell isolated and culture. Human mesenchymal stem cells (hMSCs) were obtained from the Orthopaedic Department of Shanghai Ninth People's Hospital, and were isolated and expanded as previously described.[32] Bone marrow aspirates were obtained from three donors (a 20 year-old man, 30 year-old woman, and 40 year-old man) during routine orthopedic surgical procedures, and the donors were healthy without metabolic disease, inherited illnesses, or other diseases that may affect the current study. The ethical approval was provided by the Ethical Committee of Shanghai Ninth People's Hospital (Shanghai, China) and the donors gave written informed consent before being included in the study. Briefly, after isolation from the bone marrow aspirates, the cells were cultured in α-MEM culture medium supplemented with 10% fetal bovine serum (FBS), 1% penicillin (100 U ml^{-1}), and streptomycinsulphate (100 mg ml^{-1}) (Invitrogen, Carlsbad, CA), and incubated at 37 °C in a humidified atmosphere of 5% CO_2 and 95% air, with the growth medium changed every 48 h. hMSCs passaged up to the fourth generation were used for the experiments described below. To investigate hMSC differentiation, an osteogenic medium was prepared in growth medium supplemented with 50 μM L-ascorbic acid, 10 mM glycerophosphate and 100 nM dexamethasone.

2.3.2 Cell attachment. The attachment of hMSCs on the four types of samples (TC, TC-AAC, TC-AAH, and TC-AA(C/H)$_6$) was examined using the 3-(4,5-dimethylthiazol-2-yl)-2,5-diphenyltetrazolium bromide (MTT, Sigma, St Louis, MO, USA) assay. One milliliter of cell suspension with a cell density of 5 × 10^4 cells per ml was seeded in a single well of a 48-well plate that contained one sample and was then incubated in a humidified 37 °C/5% CO_2 incubator. The cells were allowed to attach on the specimens for 4, 8, 12, and 24 h. At each

predetermined time point, 0.1 ml of MTT solution was added to each well, and the specimens were incubated at 37 °C for 4 h to form formazan, which was then dissolved using 0.5 ml dimethylsulfoxide (Sigma-Aldrich). The optical density (OD) was measured at 570 nm using an automated plate reader (Synergy HT multi-detection microplate). Similar to the above cell culture procedure, cells on the surface of the three kinds of TCs were stained with DAPI at the 12 h time point. The cells were observed using a fluorescence microscope (Nikon, Japan).

2.3.3 Cell proliferation. In the proliferation assay, the cell density of the proliferation assays was 1×10^4 cells per well, and the cells were cultured for 1, 3, and 6 days in a humidified 37 °C/5% CO_2 incubator. The number of cells at each prescribed time point was measured with MTT assay according to the process described earlier. The OD value at day 1 was measured as the baseline. The proliferation of hMSCs was expressed as the ratio of the OD value relative to the value for day 1 of the same specimen.

2.3.4 Alkaline phosphatase (ALP) activity assay. hMSCs were seeded onto the four types of samples in 48-well plates at a seeding density of 5×10^4 cells per well. After incubation with the substrates for 24 h, the culture medium was changed to the osteogenic medium, and then cultured for up to 14 d. At day 4, 7, or 14, samples were washed three times with PBS and then lysed in a 0.2% Triton X-100 solution using four freeze–thaw cycles. The ALP activity was determined using *p*-nitrophenylphosphate (*p*NPP, Sigma, St. Louis, MO) according to the procedures mentioned in the previous article.[33]

For the ALP staining assay, hMSCs were seeded onto the four types of samples in 6-well plates at a seeding density of 3×10^5 cells per well. After being cultured with the osteogenic medium for 7 days, all the specimens with cells were rinsed gently with PBS, and then the ALP staining was accomplished following the procedure in the literature.[34]

2.3.5 Quantitative real-time PCR. hMSCs were seeded onto the four specimens in 6-well plates at a seeding density of 3×10^5 cells per well. Cells were harvested after culture in osteogenic medium for 4, 7, 14, or 21 days. The osteogenic-associated gene expression of hMSCs was quantified by real-time PCR. Total RNA was isolated from hMSCs using TRIZOL (Invitrogen, Carlsbad, CA), and 1 mg of the RNA solution was converted to complementary DNA (cDNA). Quantitative real-time PCR was performed using an ABI 7500 Real-Time PCR System (Applied Biosystems, USA) with a PCR kit (SYBR Premix EX Taq, TaKaRa). The comparative C_t-value method was used to calculate the relative quantity of human alkaline phosphatase (h-ALP), type I collagen (h-COL1), osteopontin (h-OPN), and osteocalcin (h-OC). The expression of the housekeeping gene glyceraldehyde-3-phosphate dehydrogenase (h-GAPDH) was used as an internal control to normalize the results. The sequences of the forward and reverse primers for the genes presented above are shown in Table 1.

2.3.6 Alizarin red staining. After 21 days of osteoinduction, the substrates were washed three times with PBS and fixed in 3.7% formaldehyde for 1 h, and then stained with a 1% Alizarin Red (Sigma-Aldrich) solution for 45 min at room temperature. Afterwards, the cell monolayers were washed with distilled water until no more color appeared in the distilled water, and then images were obtained using a digital camera (Nikon D90, Japan). In the quantitative analysis, the stain was dissolved in 10% cetylpyridinum chloride (Sigma-Aldrich) in 10 mM sodium phosphate (pH = 7), and the absorbance values were measured at 620 nm.

Table 1 Primers used in this study[a]

Target gene	Direction	5′–3′ primer sequence
h-COL1	F	5′-CCTGAGCCAGCAGATCGAGAA-3′
	R	5′-GGTACACGCAGGTCTCACCAGT-3′
h-ALP	F	5′-TTGACCTCCTCGGAAGACACTC-3′
	R	5′-CCATACAGGATGGCAGTGAAGG-3′
h-OPN	F	5′-CTGAACGCGCCTTCTGATTG-3′
	R	5′-ACATCGGAATGCTCATTGCTCT-3′
h-OC	F	5′-GGCGCTACCTGTATCAATGGC-3′
	R	5′-TGCCTGGAGAGGAGCAGAACT-3′
h-GAPDH	F	5′-CCTGCACCACCAACTGCTTA-3′
	R	5′-AGGCCATGCCAGTGAGCTT-3′

[a] F, forward; R, reverse. h-COL1, collagen type I; h-ALP, alkaline phosphatase; h-OPN, osteopontin; h-OC, osteocalcin; h-GAPDH, glyceraldehydes-3-phosphate dehydrogenase.

2.4 *In vivo* study

2.4.1 Surgical procedure. A rabbit model with femur condyle defect was used to evaluate the *in vivo* function of the collagen-modified titanium coatings. Twenty four adult white New Zealand rabbits were obtained from Laboratory Animal Center of Shanghai Ninth People's Hospital (male, 2–2.5 kg body weight). The use of animals and the experimental protocol were approved by the Animal Experimental Ethics Committee of Ninth People Hospital, School of Medicine, Shanghai Jiao Tong University, and the surgery was performed according to the Guide of the Care and Use of Laboratory Animals published by the National Academy of Sciences. Rabbits were anesthetized by injecting 3% Nembutal (30 mg kg^{-1}) *via* the ear vein and a longitudinal incision was made by scalpel in the rabbit femur under rigorous aseptic conditions. Circular holes with 2.9 mm diameter and 10 mm deep were drilled using a surgical electronic drill and thoroughly rinsed with physiological saline to remove shards of bone. Implants of TC and TC-AAC were used in this study. The wound was sutured with nylon thread. Rabbits were sacrificed 1, 2, or 3 months after implantation.

2.4.2 Micro-X-ray computed tomography (μCT) analysis. After sacrifice, distal femurs with implants were collected under aseptic condition, fixed in 4% paraformaldehyde for 2 days, and then rinsed with running water for 24 h. For assessment of the bone architecture around the different implants after 3 months of implantation, femur condyles with implants were examined using a desk-top micro-CT (GE Locus SP), equipped with an 80 kV X-ray source with a camera pixel size of 15 μm. During scanning, the femur condyles were placed in polyethylene tubes filled with alcohol 75 volume%. Micro-CT images along the transection and midsagital planes in the region around the implant were obtained. The scans resulted in reconstructed data sets with a voxel size of 28.79 μm. To determine the trabecular volume of interest (VOI) in the axial direction, the region of interest was chosen with its closest edge at 4.0 mm

distally from the growth plate. The bone volume fraction (BV/TV), trabecular thickness (Tb.Th), trabecular separation (Tb.Sp), and trabecular number (Tb.N) were calculated as measurements of the trabecular bone mass and its distribution.

2.4.3 Fluorescence labeling of new bone formation around the implants. To assess the osteogenic activity, the fluorochromic bone marker calcein green (CG) (15 mg kg^{-1} BW; Sigma) was administered subcutaneously to all the groups before one week of the rabbits' sacrifice. Specimens were dehydrated through a series of graded ethanol solutions (50%, 60%, 75%, 85%, 95%, and 100%). The dehydrated specimens were preserved in absolute ethanol for subsequent assay. The dehydrated samples were embedded in polymethylmethacrylate resin. Undecalcified sections with a thickness of 100 μm were cut using a saw microtome (Leica ST1600). The thickness of the sections was polished to 50 mm using P300, P800, and P1200 abrasive paper, and then burnished with flannelette and abradum to 20–30 μm. Finally, the fluorescence of calcein in bone tissues surrounding the bone cement was visualized using confocal laser scanning microscopy (CLSM, Leica TCS SP2; Leica Microsystems, Heidelberg, Germany).

2.4.4 Measurement of bone-implant contact. Sections were prepared as described above. After being dipped in 1% methane acid solution for 3 min and 20% methanol solution for 2 h, sections were stained with Van Gieson's picro fuchsin, and then observed by laser scanning confocal fluorescence microscopy (Leica TCS.SP5). The bone-implant contact (BIC) was measured by image analysis software (Bioquant) according to previous reported methods.[35] BIC levels were defined as the fraction of direct bone apposition at the surface of the implant. The total perimeter observed and the total perimeter attached by bone were measured for each micrograph. Bone apposition was defined as a continuum of material from the surface of the implant to the surrounding bone. The values were the mean of the five samples.

2.5 Statistical analysis

The data were expressed as the mean ± standard deviation (SD) for all the experiments ($n = 5$) and statistical differences were determined by an analysis of variance (ANOVA). Values of $p < 0.05$ were considered to be statistically significant.

3. Results

3.1 Attachment and proliferation of hMSCs

Fig. 1 shows the attachment of hMSCs on the surface of the four samples. It was found that all of the three modified titanium coatings could improve notably the attachment of cells. At all of the time points, there was significantly more adhered cells on TC-AA(C/H)$_6$ more than on TC-AAC and TC-AAH. We also observed that within the first 12 h, the number of cells adhered on TC-AAC was more than that on TC-AAH.

The proliferation rate of hMSCs on these samples was further evaluated, and the data of the cell proliferation on the samples after 3 and 6 days were normalized to that of day 1 for calibration of the variation of the cultured cells.[6] In Fig. 2, it can be observed

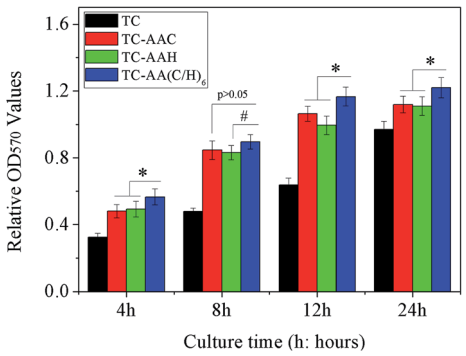

Fig. 1 Attachment of hmscs on the surface of the four samples, measured using a colorimetric mtt assay. *$p < 0.05$ denotes differences compared between TC-AA(C/H)$_6$ and the other two modified titanium coatings (TC-AAC and TC-AAH). #$p < 0.05$ denotes difference compared between TC-AA(C/H)$_6$ and TC-AAH at 8 h.

that the cells on TC-AA(C/H)$_6$ exhibited a higher proliferation rate compared with that on the other two modified titanium coatings, and the difference was significant. Furthermore, the proliferation rate of cells on TC-AAH was higher than that on TC-AAC.

3.2 Osteogenic differentiation of hMSCs

In order to evaluate the osteogenic differentiation of hMSCs on the four kinds of specimens, ALP activity assay, real-time PCR, and Alizarin red staining were performed, and the results are shown in Fig. 3. From the results of the quantification of ALP activity (Fig. 3(A)), it can be seen that after osteogenic induction, hMSCs on TC-AA(C/H)$_6$ exhibited significantly higher ALP activity relative to the other two modified titanium coatings (TC-AAC and TC-AAH) at days 4, 7, and 14. Consistent with this observation, the ALP staining on TC-AA(C/H)$_6$ was significantly more distinct than that on TC-AAC and TC-AAH (Fig. 3(B)). In the real-time PCR assay, TC-AA(C/H)$_6$ also exhibited significantly promoted levels of h-COL1 (Fig. 4(a)), h-ALP (Fig. 4(b)), h-OPN (Fig. 4(c)), and h-OC (Fig. 4(d)) mRNA expression compared with TC-AAC and TC-AAH at most of the time points, such as day 4, 7, and 14 of h-COL1, day 7 and 14 of h-ALP and

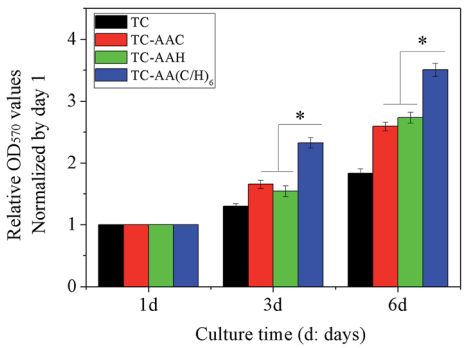

Fig. 2 Proliferation of hmscs on the surface of the four different samples. The relative proliferation rate of hmscs, measured by od values at days 3 and 6, were normalized to day 1. *$p < 0.05$ denotes differences compared between TC-AA(C/H)$_6$ and the other two modified titanium coatings (TC-AAC and TC-AAH).

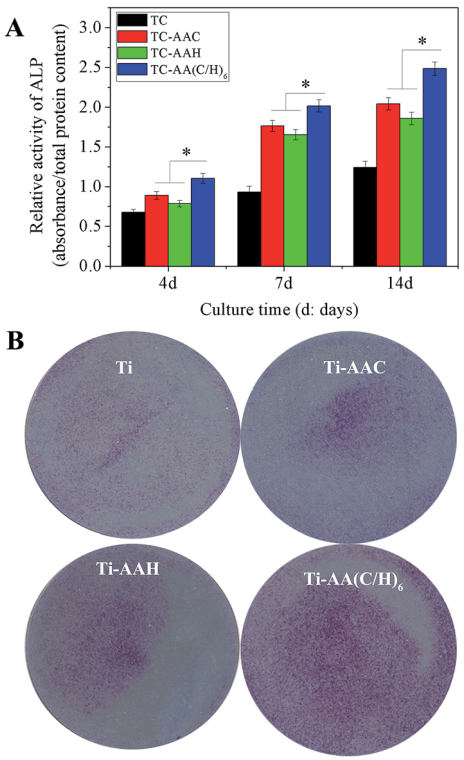

Fig. 3 Quantification of the alp activity after 4, 7, and 14 days of osteogenic induction (A) and alp staining performed at day 7 (B). *p < 0.05 denotes differences compared between TC-AA(C/H)$_6$ and the other two modified titanium coatings (TC-AAC and TC-AAH).

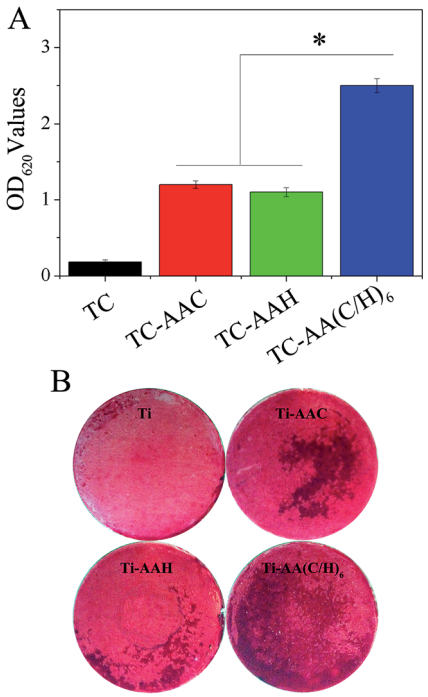

Fig. 5 Mineralization (Alizarin red staining) assay. (A) Colorimetric quantitative analysis of the extracellular matrix mineralization on the samples after 21 days of incubation. *p < 0.05 denotes differences compared between TC-AA(C/H)$_6$ and the other two modified titanium coatings (TC-AAC and TC-AAH). (B) Alizarin red staining showing that mineralization was consistent with a quantitative analysis of mineralization.

h-OPN, and day 14 and 21 of h-OC. As shown in Fig. 5(B), the extracellular matrix mineralization on the surface of TC-AA(C/H)$_6$ was obviously more than that of the other three specimens. According to the quantitative results from Fig. 5(A), the OD value of TC-AA(C/H)$_6$ was more than twice that of TC-AAC and TC-AAH. In addition, the ability of promoting

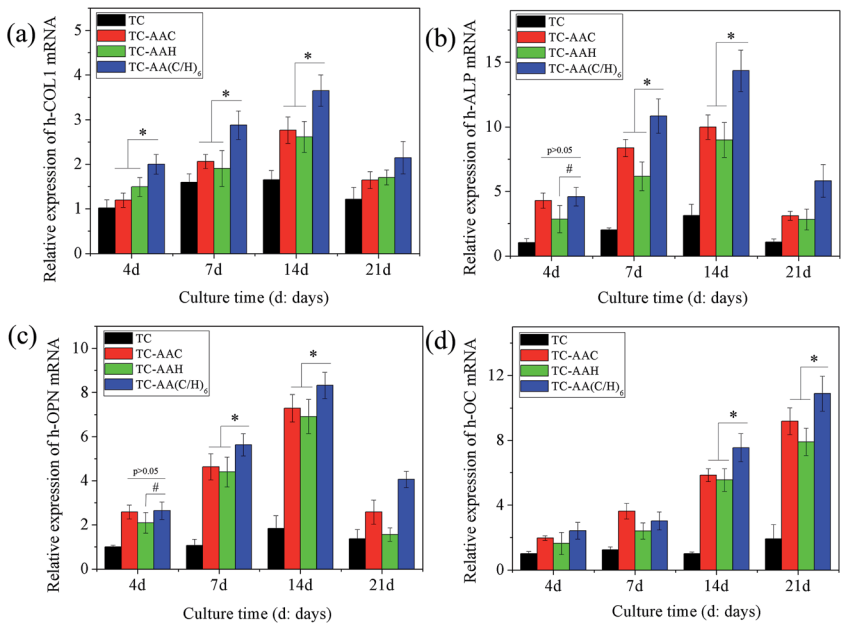

Fig. 4 Comparison of osteogenesis-related gene expression as determined by real-time pcr. *p < 0.05 denotes differences compared between TC-AA(C/H)$_6$ and the other two modified titanium coatings (TC-AAC and TC-AAH); #p < 0.05 denotes difference compared between TC-AA(C/H)$_6$ and TC-AAH.

osteogenic differentiation of TC-AAC was better than that of TC-AAH, according to the results of ALP activity, real-time PCR, and Alizarin red staining.

3.3 Micro-CT image analysis

Fig. 6(A) shows the micro-CT images along the transection and midsagital planes in the region around the implants after 3 months of implantation. It can be obviously found that the trabecular around TC-AA$(C/H)_6$ was more than that around TC-AAC and TC-AAH. The four parameters of the trabecular volume of interest (VOI, 3.4 mm) in the axial direction were also studied. BV/AV (Fig. 6(B)) and Tb.N (Fig. 6(D)) of TC-AA$(C/H)_6$ were 11.2590 ± 0.8453% and 1.8359 ± 0.1246 mm^{-3}, respectively, which were significantly higher than that of TC-AAC (9.3825 ± 0.8386% and 1.3387 ± 0.0729 mm^{-3}, $p < 0.05$) and

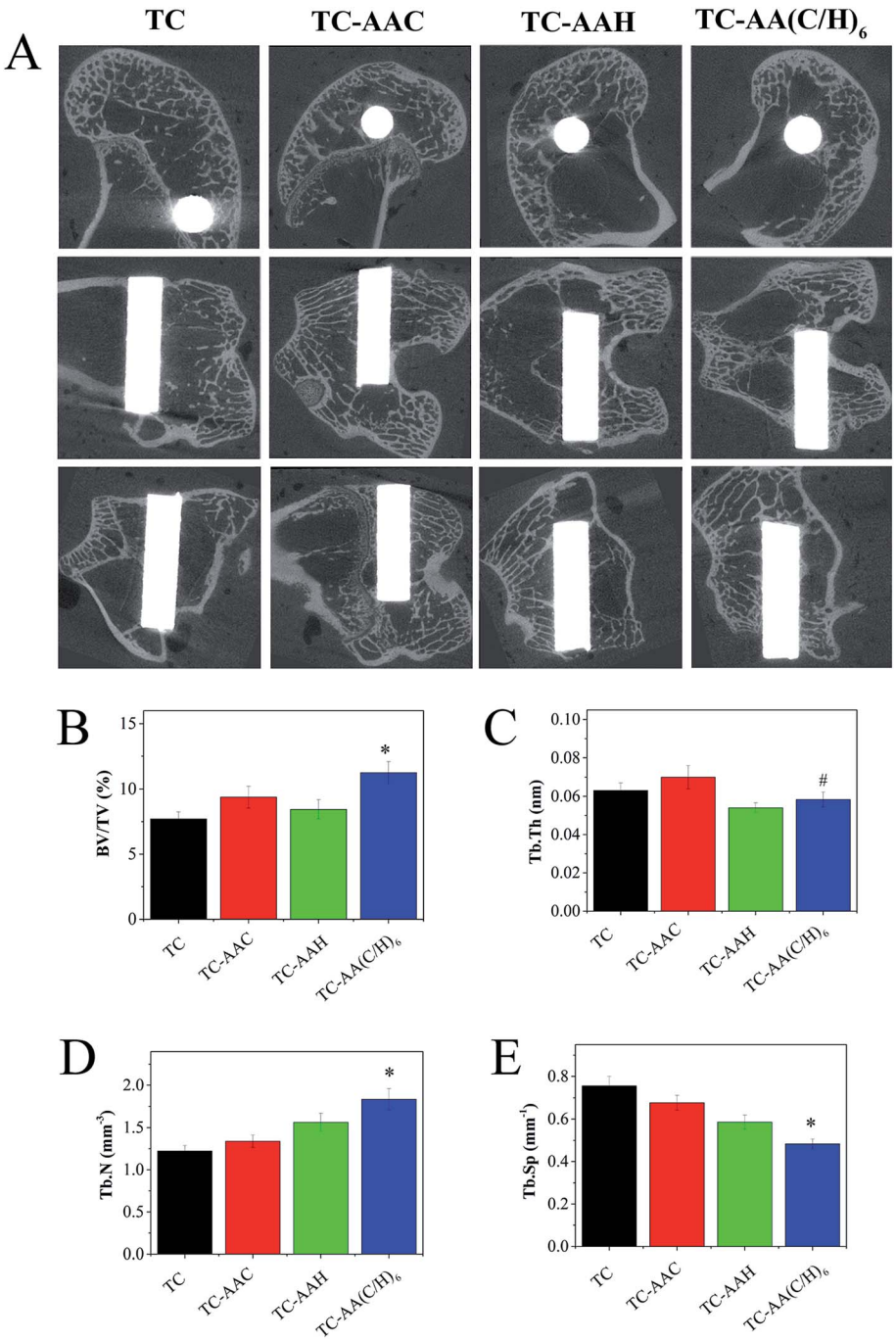

Fig. 6 Micro-CT images along the transection and midsagital planes in the region around implants after 3 months of implantation (A), and the four kinds of microstructural parameters of the trabecular volume of interest (VOI) in the axial direction: BV/TV (B), Tb.Th (C), Tb.N (D), and Tb.Sp (E). *$p < 0.05$ denotes differences compared between TC-AA$(C/H)_6$ and the other three samples. #$p < 0.05$ denotes difference compared between TC-AA$(C/H)_6$ and TC-AAC.

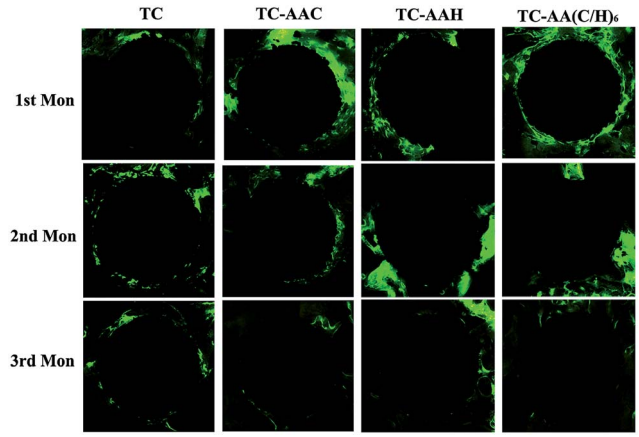

Fig. 7 Confocal laser scanning micrograph showing the green fluorescence labeling of calcein in the newly formed bone around the implant in the four groups.

TC-AAH (8.4424 ± 0.7279% and 1.5632 ± 0.1057 mm^{-3}, $p < 0.05$). Tb.Sp (Fig. 6(E)) of TC-AA(C/H)$_6$ was 0.4833 ± 0.0232 mm^{-1}, which was less than that of TC-AAC and TC-AAH (0.6769 ± 0.0348 mm^{-1} and 0.5857 ± 0.0329 mm^{-1}, respectively, $p < 0.05$). As for Tb.Th (Fig. 6(C)), that of TC-AA(C/H)$_6$ was 0.0583 ± 0.0039 nm, which was greater than the 0.0540 ± 0.0026 nm of TC-AAH but smaller than the 0.0700 ± 0.0061 nm of TC-AAC.

3.4 Fluorescence micrograph of new bone formation around the implants

The bright green fluorescence labeling of calcein in the newly formed bone surrounding the two kinds of implants is shown in Fig. 7. In the first month, little green fluorescence was found around the surface of TC, while there was much green fluorescence around all of the three modified titanium coatings, and the green fluorescence around TC-AA(C/H)$_6$ was more than that around TC-AAC and TC-AAH. In the second month, much more green fluorescence appeared around TC, while there were also much around TC-AAC and TC-AAH. However, the green

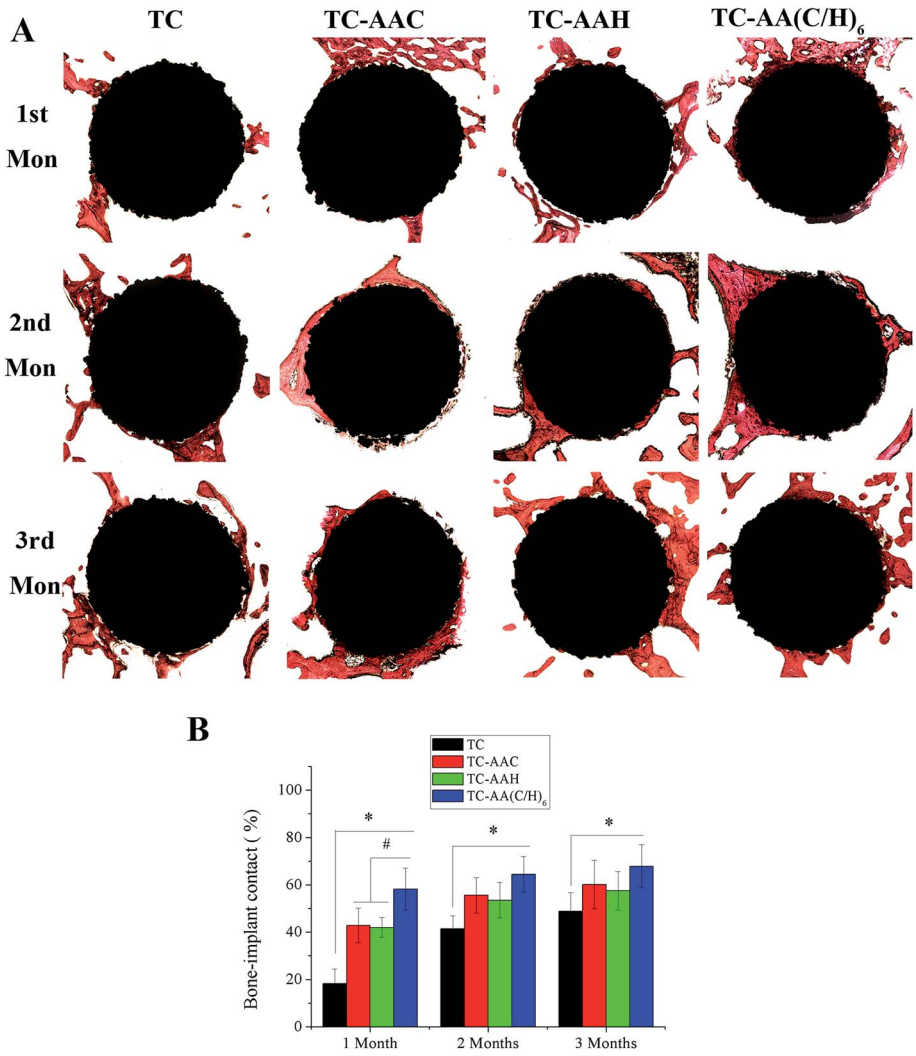

Fig. 8 (A) Histological morphology of the interface between implants and bone tissue after 1 month, 2 months, and 3 months implantation in rabbit femur condyles. (B) Percentages of the measured bone-implant contact of the titanium coating-based implants ($n = 5$).

fluorescence around TC-AA(C/H)$_6$ became much less. In the third month, there was still some green fluorescence around TC; however, there was no green fluorescence found around the three modified titanium coatings. These results indicate that the modified titanium coatings could improve early osseointegration of implants and shorten the osseointegration time. Obviously, the early osseointegration of TC-AA(C/H)$_6$ was the best.

3.5 Histological observations and bone-implant contact

Fig. 8 shows the histological appearance of the implants and bone after 1, 2, and 3 months of implantation and percentages of the measured bone-implant contact of implants. From Fig. 8(A), it can be seen that, unlike TC, new bones could be found on the three modified titanium coatings in the first month, and that on TC-AA(C/H)$_6$ is more than that on TC-AAC and TC-AAH. After three months growth, although the TC implant was surrounded by much bone, there were many gaps between the TC implant and new bone tissues. However, three modified titanium coatings were closed when combined with bone. The results of the bone-implant contact measurements are summarized in Fig. 8(B). It can be seen that the bone-implant contact of TC-AA(C/H)$_6$ implants is higher than that of TC-AAC and TC-AAH implants at all the time points. In particular, the difference between TC-AA(C/H)$_6$ and the two others (TC-AAC and TC-AAH) is significant. Furthermore, the BIC of the TC-AA(C/H)$_6$ implants is significantly higher than that of the TC implants at all the time points.

4. Discussion

Biomacromolecules are a kind of special biomaterials that not only possess excellent bioactivity but also act as biological cues for adherent cells, compared with metallic, ceramic, and other macromolecule materials.[2] Therefore, biomacromolecules, especially the components of ECM, are gaining increasing favor from material scientists. Some biomacromolecules have been blended with ceramics,[36] grafted on polymer materials,[37] or used in metal materials surface modification.[38] Type I collagen and hyaluronic acid, both as the main components of ECM, play respective roles in the ECM system and take part in regulating a cell's behaviors. Type I collagen and hyaluronic acid are often employed for the same material.[39,40] In our previous study, type I collagen and hyaluronic acid also have been used to modify titanium coating by layer-by-layer covalent immobilization. However, few reports in the literature have investigated the synergistic effects between type I collagen and hyaluronic acid on osteointegration. Therefore, in this work, the synergistic effects between type I collagen and hyaluronic acid in Col/HA-multilayer-modified titanium coatings was investigated.

In vitro, hMSCs were employed to compare the cytocompatibility of the three modified titanium coatings and unmodified titanium coatings. Although TC-AAC and TC-AAH possess favorable properties to improve a cell's adhesion, proliferation, and differentiation, Col/HA-multilayer-modified titanium coatings showed the best effect of promotion. These results indicated that a synergistic effect exists between type I collagen and hyaluronic acid on cytocompatibility. Type I collagen is the most abundant protein in bone and the main component of ECM. Like fibronectin and laminin, type I collagen also has an abundance of the amino acid sequence arginine–glycine–asparagine (RGD). RGD is recognized by the integrin receptors located at the cell membrane, which could stimulate a cell's adhesion and further trigger proliferation and differentiation.[41,42] On the other hand, hyaluronic acid is the major ligand of CD44, which is a multifunctional and multistructural receptor.[43] Ouasti *et al.*[44] found that the introduction of RGD peptides on the hydroxyapatite backbone allows modulation of the uptake of the polysaccharide through the binding to both CD44 and integrins. This is further evidence of the synergistic effect between type I collagen and hyaluronic acid. Furthermore, because of its carboxy groups, HA possesses high water sorption and retention capacity and viscoelasticity, which contribute to cell migration and proliferation.[45] Therefore, it can be found that the proliferation rate of TC-AAH at 6 days was higher than that of TC-AAC, and the proliferation rate of TC-AA(C/H)$_6$ was obviously higher than that of TC-AAC and TC-AAH (Fig. 2). As for cell differentiation, Viale-Bouroncle *et al.*[15] reported that type I collagen induced independently the expression of the osteogenic differentiation markers ALP and OPN *via* the FaK and ERK signaling pathways. Kawano *et al.*[46] found that hyaluronic acid enhanced BMP-2 osteogenic bioactivity in MG63 cells *via* a downregulation of BMP-2 antagonists and ERK phosphorylation. Thereby, the synergistic effects of type I collagen and hyaluronic acid may be a better downregulated ERK phosphorylation and promotion of osteogenesis of hMSCs.

The synergistic effect of type I collagen and hyaluronic acid on osseointegration was further confirmed *in vivo*. The results of micro-CT indicated that the osseointegration of the TC-AA(C/H)$_6$ group was distinctly better than that of the TC-AAC and TC-AAH groups (Fig. 6). From the results of the four parameters of the VOI, it can be found that type I collagen may contribute to the trabecular thickness while hyaluronic acid may be beneficial to the increase in the trabecular number, the mechanism of which should be explored by further experiments. When combining type I collagen and hyaluronic acid, the TC-AA(C/H)$_6$ group demonstrated the highest bone volume fraction, the greatest trabecular number, and the lowest trabecular separation among all the groups. Meanwhile, the early osseogenetic activity of the TC-AA(C/H)$_6$ group was strongest among all the groups (Fig. 7) and the early bone-implant contact of TC-AA(C/H)$_6$ group was highest (Fig. 8). All the results from the *in vivo* study confirmed the synergistic effect of type I collagen and hyaluronic acid in osteogenesis. The synergistic effect of type I collagen and hyaluronic acid also exists in other tissue repair. For example, Matsiko *et al.*[47] found that the addition of hyaluronic acid could improve cellular infiltration and promote the early-stage chondrogenesis of collagen-based scaffold.

5. Conclusion

This paper investigated the synergistic effect between type I collagen and hyaluronic acid in Col/HA-multilayer-modified

titanium coatings. *In vitro*, the adhesion, proliferation, and differentiation of hMSCs on TC-AA$(C/H)_6$ were obviously better than that on TC-AAC and TC-AAH. *In vivo*, TC-AA$(C/H)_6$ possessed the fastest osseointegration rate, the best early osseointegration, and the biggest bone-implant contact compared with TC-AAC and TC-AAH. All the results indicated that there exists favorable synergistic effects of type I collagen and hyaluronic acid in TC-AA$(C/H)_6$ on its biological properties.

Acknowledgements

This work is supported by the National Natural Science Foundation of China (Grant No. 81501856 and 31271015), grant awarded by Biomedical Engineering crossover project of Shanghai JiaoTong University (YG2014ZD01), and the Opening Project of the Key Laboratory of Inorganic Coating Materials, Chinese Academy of Sciences (KLICM-2014-04).

References

1 C. D. Gildner, D. C. Roy, C. S. Farrar and D. C. Hocking, *Matrix Biol.*, 2014, **34**, 33–45.
2 H. K. Kleinman, D. Philp and M. P. Hoffman, *Curr. Opin. Biotechnol.*, 2003, **14**, 526–532.
3 R. O. Hynes, *Science*, 2009, **326**, 1216–1219.
4 J. E. Meredith, J. B. Fazeli, Jr and M. A. Schwartz, *Mol. Biol. Cell*, 1993, **4**, 953–961.
5 C. J. Sobers, S. E. Wood and M. Mrksich, *Biomaterials*, 2015, **52**, 385–394.
6 H. Tan, S. Guo, S. Yang, X. Xu and T. Tang, *Acta Biomater.*, 2012, **8**, 2166–2174.
7 K. Thomas, A. J. Engler and G. A. Meyer, *Connect. Tissue Res.*, 2015, **56**, 1–8.
8 Y. Xu, G.-y. Xu, C. Tang, B. Wei, X. Pei, J.-c. Gui, B.-H. Min, C.-z. Jin and L.-m. Wang, *J. Biomed. Mater. Res., Part B*, 2015, **103**, 670–678.
9 E. E. Antoine, P. P. Vlachos and M. N. Rylander, *Tissue Eng., Part B*, 2014, **20**, 683–696.
10 A. E. Sorkio, E. P. Vuorimaa-Laukkanen, H. M. Hakola, H. Liang, T. A. Ujula, J. J. e. Valle-Delgado, M. €Osterberg, M. L. Yliperttula and H. Skottman, *Biomaterials*, 2015, **51**, 257–269.
11 M. Y. Zhao, *eXPRESS Polym. Lett.*, 2014, **8**, 322–335.
12 R. Müller, J. Abke, E. Schnell, F. Macionczyk, U. Gbureck, R. Mehrl, Z. Ruszczak, R. Kujat, C. Englert, M. Nerlich and P. Angele, *Biomaterials*, 2005, **26**, 6962–6972.
13 M. Heller, P. W. Kämmerer, B. Al-Nawas, M.-A. Luszpinski, R. Förch and J. Brieger, *J. Biomed. Mater. Res., Part A*, 2015, **103**, 2035–2044.
14 E. Ruoslahti and M. D. Pierschbacher, *Science*, 1987, **238**, 491–497.
15 S. Viale-Bouroncle, M. Gosau and C. Morsczeck, *Arch. Oral Biol.*, 2014, **59**, 1249–1255.
16 G. A. D. Lullo, S. M. Sweeney, J. Korkko, L. Ala-Kokko and J. D. S. Antonio, *J. Biol. Chem.*, 2002, **277**, 4223–4231.
17 B. D. Bezerra, M. A. M. Brazao, M. L. G. de Campos, M. Z. Casati, E. A. Sallum and A. W. Sallum, *Clin. Oral. Implants. Res.*, 2012, **23**, 938–942.
18 A. K. Jha, X. Xu, R. L. Duncan and X. Jia, *Biomaterials*, 2011, **32**, 2466–2478.
19 R. Pradhan, T. Ramasamy, J. Y. Choi, J. H. Kim, B. K. Poudel, J. W. Tak, N. Nukolova, H.-G. Choi, C. S. Yong and J. O. Kim, *Carbohydr. Polym.*, 2015, **123**, 313–323.
20 J. A. Burdick and G. D. Prestwich, *Adv. Mater.*, 2011, **23**, H41–H56.
21 X. Duan, X. Zhu, X. Dong, J. Yang, F. Huang, S. Cen, F. Leung, H. Fan and Z. Xiang, *Mater. Sci. Eng., C*, 2013, **33**, 3951–3957.
22 Z. Chen, S. Deng, D. Yuan, K. Liu, X. Xiang and G. Feng, *Tissue Eng., Part A*, 2015, **21**, S160–S161.
23 A. K. Jha, A. Mathur, F. L. Svedlund, J. Ye, Y. Yeghiazarians and K. E. Healy, *J. Controlled Release*, 2015, **209**, 308–316.
24 M. Long and H. J. Rack, *Biomaterials*, 1998, **19**, 1621–1639.
25 C. Jaeggi, R. Mooser, V. Frauchiger and P. Wyss, *Mater. Lett.*, 2009, **63**, 2643–2645.
26 C. Treves, M. Martinesi, M. Stio, A. Gutierrez, J. A. Jimenez and M. F. Lopez, *J. Biomed. Mater. Res., Part A*, 2010, **92**, 1623–1634.
27 D. A. Puleo and A. Nanci, *Biomaterials*, 1999, **20**, 2311–2321.
28 H. Ao, Y. Xie, H. Tan, S. Yang, K. Li, X. Wu, X. Zheng and T. Tang, *J. R. Soc., Interface*, 2013, **10**, 20130070.
29 H.-Y. Ao, Y.-T. Xie, S.-B. Yang, X.-D. Wu, K. Li, X.-B. Zheng and T.-T. Tang, *J. Orthop. Translat.*, 2016, **5**, 16–25.
30 H. Ao, Y. Xie, A. Qin, H. Ji, S. Yang, L. Huang, X. Zheng and T. Tang, *J. Biomater. Sci., Polym. Ed.*, 2014, **25**, 1211–1224.
31 H. Ao, Y. Xie, H. Tan, X. Wu, G. Liu, A. Qin, X. Zheng and T. Tang, *J. Biomed. Mater. Res., Part A*, 2014, **102**, 204–214.
32 T. T. Tang, H. Lu and K. R. Dai, *Mater. Sci. Eng., C*, 2002, **20**, 57–61.
33 F. Yang, Y. Xie, H. Li, T. Tang, X. Zhang, Y. Gan, X. Zheng and K. Dai, *J. Biomed. Mater. Res., Part B*, 2010, **95**, 192–201.
34 N. Bock, A. Riminucci, C. Dionigi, A. Russo, A. Tampieri, E. Landi, V. A. Goranov, M. Marcacci and V. Dediu, *Acta Biomater.*, 2010, **6**, 786–796.
35 X.-W. Yu, X.-H. Xie, Z.-F. Yu and T.-T. Tang, *J. Biomed. Mater. Res., Part B*, 2009, **89**, 36–44.
36 M.-H. Lee, C. You and K.-H. Kim, *Materials*, 2015, **8**, 1150–1161.
37 M. Drobota, L. M. Gradinaru, C. Ciobanu and I. Stoica, *J. Adhes. Sci. Technol.*, 2015, **29**, 2208–2219.
38 M. Sartori, G. Giavaresi, A. Parrilli, A. Ferrari, N. N. Aldini, M. Morra, C. Cassinelli, D. Bollati and M. Fini, *Int. Orthop.*, 2015, **39**, 2041–2052.
39 L. A. S. Callahan, A. M. Ganios, D. L. McBurney, M. F. Dilisio, S. D. Weiner, W. E. Horton and M. L. Becker, *Biomacromolecules*, 2012, **13**, 1625–1631.
40 Y. Huang, Q. Luo, X. Li, F. Zhang and S. Zhao, *Acta Biomater.*, 2012, **8**, 866–877.
41 T. Re'em, O. Tsur-Gang and S. Cohen, *Biomaterials*, 2010, **31**, 6746–6755.
42 U. Hersel, C. Dahmen and H. Kessler, *Biomaterials*, 2003, **24**, 4385–4415.
43 A. Avigdor, *Blood*, 2004, **103**, 2981–2989.

44 S. Ouasti, P. J. Kingham, G. Terenghi and N. Tirelli, *Biomaterials*, 2012, **33**, 1120–1134.
45 Y. Lei, S. Gojgini, J. Lam and T. Segura, *Biomaterials*, 2011, **32**, 39–47.
46 M. Kawano, W. Ariyoshi, K. Iwanaga, T. Okinaga, M. Habu, I. Yoshioka, K. Tominaga and T. Nishihara, *Biochem. Biophys. Res. Commun.*, 2011, **405**, 575–580.
47 A. Matsiko, T. J. Levingstone, F. J. O'Brien and J. P. Gleeson, *J. Mech. Behav. Biomed. Mater.*, 2012, **11**, 41–52.